Analytical calculation of the longitudinal electric field resulting from the tight focusing of an ultrafast transverse-magnetic laser beam

Charles Varin and Michel Piché

Centre d'Optique, Potonique et Laser, Université Laval, Québec G1K 7P4, Canada

Miguel A. Porras

Departemento de Física Aplicada, Escuela Técnica Superior de Ingenerios de Minas, Universidad Politécnica de Madrid, Rios Rosas 21, E-28003 Madrid, Spain

Received July 27, 2005; revised February 6, 2006; accepted February 6, 2006; posted February 10, 2006 (Doc. ID 63685)

A purely time-domain approach is proposed for the propagation of vectorial ultrafast beams in free space beyond the paraxial and the slowly varying envelope approximations. As an example of application of this method, we describe in detail the vectorial properties of an ultrafast tightly focused transverse-magnetic (TM_{01}) beam, where special attention is given to the longitudinal electric field component. We show that for spot sizes at the waist comparable to the wavelength, the beam diverges more rapidly than expected from paraxial theory. A consequence of this phenomenon is a faster decrease of the amplitude of the longitudinal field away from the waist and a faster evolution of the axial Gouy phase shift in the vicinity of the focus. It has been observed that the phase of the beam has an overall variation of 2π from $z=-\infty$ to ∞, independent of the beam spot size at the waist and pulse duration.

OCIS codes: 260.2110, 320.5550, 350.5500.

1. INTRODUCTION

There is a growing interest for radially polarized transverse-magnetic optical beams due to the fact that they can be focused to a tighter spot size than the fundamental TEM_{00} Gaussian beam mode.[1] It has been demonstrated by Dorn *et al.* that this particular property is explained by the presence of a longitudinal electric field component along the axis of the beam.[2] In general, papers dealing with radially polarized transverse-magnetic modes, whose lowest-order mode is known as the TM_{01} mode,[3] do not provide much detail regarding the corrections associated with a finite pulse duration. In fact, temporal effects due to ultrashort pulse durations may have important implications for several applications such as two-photon microscopy and acceleration of electrons in free space (see, for example, Ref. 4).

In this paper, we give a complete vectorial description of an ultrafast tightly focused TM_{01} laser beam in free space, where analytical calculations are simultaneously made beyond the paraxial and the slowly varying envelope approximations (PaSVEAs). We show that the results obtained via the time-domain method we propose are consistent with the experimental results of Dorn *et al.*,[2] where it is shown that, when a TM_{01} beam is strongly focused, a narrow peak of intensity appears along the optical axis. We give evidence that this effect is due to the transfer of power from the transverse electric and magnetic components to the longitudinal electric component of the beam. We show that, along the axis, the properties of the longitudinal field of a strongly focused ultrashort TM_{01} beam differ from what is predicted by paraxial theory; significant modifications of the group velocity, of the carrier frequency, and of the divergence of the beam are observed. It is also demonstrated that the global variation of the phase of the longitudinal field along the axis, i.e., the axial Gouy phase shift, is of 2π from $z=-\infty$ to ∞ and does not depend on the beam spot size at the waist or the pulse duration. The method used is general and could also be applied to the fundamental Gaussian beam and to higher-order modes as well. It should be noted that our analysis is carried out without resorting to Fourier transforms.

The paper is divided as follows. In Section 2 we propose a general method to obtain the corrections to paraxial monochromatic beams purely in the time domain. In Section 3 we apply this method to evaluate the corrections to an ultrafast tightly focused TM_{01} laser beam and we expose in detail the features of its axial longitudinal field, including the axial Gouy phase shift. Finally, in Section 4 we compare this work with related published works.

2. TIME-DOMAIN APPROACH TO THE PROPAGATION OF ULTRAFAST NONPARAXIAL BEAMS

State-of-the-art mode-locked laser oscillators can generate ultrafast pulses whose duration can be as short as a few optical cycles.[5] Such pulses—with a finite spatiotemporal extent—can in principle be isolated, amplified, temporally compressed, and spatially focused to reach extreme field intensities within a volume that is of the order of the third power of the laser wavelength. In that situa-

tion, the commonly used PaSVEAs do not apply directly and must be corrected. We propose here a time-domain method to solve the problem of ultrafast nonparaxial vectorial beam propagation in free space where the full solution of Maxwell's equations proceeds in three steps: (1) a perturbed form of the paraxial wave equation is solved, (2) the longitudinal electric field is obtained from the free-space divergence equation of the electric field, and (3) the magnetic flux is obtained from the differential form of Ampère's law. This analysis, made beyond the PaSVEAs, is presented in the following subsections.

A. Perturbed Paraxial Wave Equation

In free space, the electric field vector $\mathbf{E}$ of a given light beam must be a solution of the vectorial wave equation

$$\nabla^2\mathbf{E} - \frac{1}{c^2}\partial_t^2\mathbf{E} = 0, \tag{1}$$

where c is the speed of light *in vacuo* and ∂_t stands for the partial derivative $\partial/\partial t$. The electric field vector is defined as follows in phasor notation:

$$\mathbf{E} = \mathrm{Re}[\tilde{\mathbf{E}}\exp[j(\omega_0 t - k_0 z)]], \tag{2}$$

with $\tilde{\mathbf{E}}$ being the complex envelope of the electric field vector and $j=\sqrt{-1}$. Also, we define $\omega_0 = k_0 c$, $k_0 = 2\pi/\lambda_0$, and λ_0 as, respectively, the central angular frequency, the central wavenumber, and the central wavelength of the wave packet spectrum. When Eqs. (1) and (2) are combined, the following equation is obtained:

$$\nabla_\perp^2\tilde{\mathbf{E}} - 2jk_0\partial_z\tilde{\mathbf{E}} - 2j\frac{\omega_0}{c^2}\partial_t\tilde{\mathbf{E}} + \partial_z^2\tilde{\mathbf{E}} - \frac{1}{c^2}\partial_t^2\tilde{\mathbf{E}} = 0, \tag{3}$$

where $\nabla_\perp$ is a differential operator acting in the transverse plane (perpendicular to the z axis).

The use of the retarded time $t' = t - z/c$ instead of the (normal) time t is sometimes preferred when dealing with the propagation of electromagnetic signals of finite spatiotemporal extent.[6] By doing so, the transverse envelope subject to diffraction is separated from the temporal envelope (pulse shape). After some manipulations, the result given in Eq. (3) can be expressed in terms of the retarded variables $t' = t - z/c$ and $z' = z$ as follows:

$$\nabla_\perp^2\tilde{\mathbf{E}} - 2jk_0\partial_{z'}\tilde{\mathbf{E}} + \partial_{z'}^2\tilde{\mathbf{E}} - \frac{2}{c}\partial_{z'}\partial_{t'}\tilde{\mathbf{E}} = 0. \tag{4}$$

Alternatively, Eq. (4) can be written in this more compact form:

$$\nabla_\perp^2\tilde{\mathbf{E}} - 2jk_0\partial_{z'}[1-\Theta]\tilde{\mathbf{E}} = 0, \tag{5}$$

with $\Theta = j(\omega_0^{-1}\partial_{t'} - (2k_0)^{-1}\partial_{z'})$. Except for the parameter Θ, one here recognizes the well-known paraxial wave equation.[3] Effectively, for paraxial and quasi-monochromatic optical beams, the term $\Theta\tilde{\mathbf{E}}$ is vanishingly small compared with the complex field $\tilde{\mathbf{E}}$ itself, i.e., $\tilde{\mathbf{E}} - \Theta\tilde{\mathbf{E}} \simeq \tilde{\mathbf{E}}$. However, for the case of an ultrafast tightly focused beam, $\Theta\tilde{\mathbf{E}}$ can no longer be neglected. It has been pointed out that the magnitude of this contribution remains small even for strongly focused single-cycle light pulses.[7–10] Thus, we can consider Eq. (5) as a perturbed paraxial wave equation.

A solution to Eq. (5) is found by expanding the envelope of the electric field vector $\tilde{\mathbf{E}}$ as a power series of Θ, i.e.,

$$\tilde{\mathbf{E}} = \sum_{n=0}^{\infty}\Theta^n\tilde{\boldsymbol{\Psi}}^{(n)}. \tag{6}$$

Then, after substituting Eq. (6) in Eq. (5) and equating terms with identical powers of Θ, the two following equations are found:

$$\nabla_\perp^2\tilde{\boldsymbol{\Psi}}^{(0)} - 2jk_0\partial_{z'}\tilde{\boldsymbol{\Psi}}^{(0)} = 0, \tag{7a}$$

$$\nabla_\perp^2\tilde{\boldsymbol{\Psi}}^{(n)} - 2jk_0\partial_{z'}\tilde{\boldsymbol{\Psi}}^{(n)} + 2jk_0\partial_{z'}\tilde{\boldsymbol{\Psi}}^{(n-1)} = 0. \tag{7b}$$

We thus notice that the term of order 0 $\tilde{\boldsymbol{\Psi}}^{(0)}$ is a solution of the paraxial wave equation. For $n>0$, the contribution of order n is obtained recursively from the order $(n-1)$. A general solution of Eq. (7b) may be written as follows (see Porras[8]):

$$\tilde{\boldsymbol{\Psi}}^{(n)} = \partial_{z'}^{n-1}\left(\frac{z'^n}{n!}\partial_{z'}\tilde{\boldsymbol{\Psi}}^{(0)}\right), \tag{8}$$

giving $\tilde{\boldsymbol{\Psi}}^{(n)}$ in terms of successive derivatives of $\tilde{\boldsymbol{\Psi}}^{(0)}$. Combining Eqs. (6) and (8), the complex envelope of the electric field vector thus reads

$$\tilde{\mathbf{E}} = \sum_{n=0}^{\infty} j^n\left(\frac{1}{\omega_0}\partial_{t'} - \frac{1}{2k_0}\partial_{z'}\right)^n\partial_{z'}^{n-1}\left(\frac{z'^n}{n!}\partial_{z'}\tilde{\boldsymbol{\Psi}}^{(0)}\right). \tag{9}$$

Through the definition of Eq. (2), the result obtained in Eq. (9) is an analytical solution of the wave equation [Eq. (1)], which holds for ultrafast nonparaxial beams.

B. Longitudinal Electric Field

In addition to the wave equation, the electric field vector must obey the divergence equation $\nabla\cdot\mathbf{E}=0$ in free space. For a given distribution of the transverse electric field vector $\mathbf{E}_\perp$, the longitudinal electric field E_z is obtained by the formal inversion of the divergence equation.[4,11] This requires the use of the complex notation defined in Eq. (2). In terms of the retarded variables t' and z', the complex envelope of the longitudinal field is given by the following expression:

$$\tilde{E}_z = \sum_{m=0}^{\infty}\sum_{n=0}^{\infty} j^{m+n}\left(\frac{1}{\omega_0}\partial_{t'} - \frac{1}{k_0}\partial_{z'}\right)^m \times\left(\frac{1}{\omega_0}\partial_{t'} - \frac{1}{2k_0}\partial_{z'}\right)^n\partial_{z'}^{n-1}\left(\frac{z'^n}{n!}\partial_{z'}\tilde{E}_z^{(0)}\right), \tag{10}$$

where $\tilde{E}_z^{(0)} = (-j/k_0)(\nabla_\perp\cdot\tilde{\boldsymbol{\Psi}}_\perp^{(0)})$ is the paraxial and slowly varying envelope of the longitudinal electric field.

C. Magnetic Flux

A general equation giving the magnetic flux vector $\mathbf{B}$ of an arbitrary ultrafast beam can be deduced from Maxwell's equations. That is, to a given distribution and polarization of the transverse electric field vector there corresponds a longitudinal electric component (see Subsection

2.B) and a magnetic flux. As an example, let us consider the case of a pulsed TM_{01} beam whose transverse electric field is radially polarized, i.e., $\mathbf{E}_\perp = E_r \mathbf{a}_r$ and $E_\theta = 0$, where r and θ are polar coordinates in the plane perpendicular to the propagation axis (the z axis). The intensity profile of this particular type of beam is characterized in the paraxial approximation by an angularly symmetric ($\partial_\theta \mathbf{E}_\perp = 0$) bright ring (its intensity is 0 at $r=0$).[3] Going through the calculation of the magnetic flux, from Ampère's law ($\nabla \times \mathbf{B} = c^{-2}\partial_t \mathbf{E}$), we obtain the following equations:

$$B_r = 0, \tag{11a}$$

$$B_z = 0, \tag{11b}$$

$$-\partial_z B_\theta = c^{-2}\partial_t E_r, \tag{11c}$$

$$r^{-1}\partial_r (r B_\theta) = c^{-2}\partial_t E_z. \tag{11d}$$

If Eqs. (11c) and (11d) are combined, we obtain the divergence equation that we solved earlier in Eq. (10). Thus, the solution of Eq. (11c) ensures that Eq. (11d) is also respected. If we express the fields in complex notation and in terms of the retarded variables, the formal inversion of Eq. (11c) yields

$$\tilde{B}_\theta = \sum_{p=0}^{\infty}\sum_{n=0}^{\infty} j^{p+n}\left(\frac{1}{\omega_0}\partial_{t'} - \frac{1}{k_0}\partial_{z'}\right)^p \left(1 - \frac{j}{\omega_0}\partial_{t'}\right) \times \left(\frac{1}{\omega_0}\partial_{t'} - \frac{1}{2k_0}\partial_{z'}\right)^n \partial_{z'}^{n-1}\left(\frac{z'^n}{n!}\partial_{z'}\tilde{B}_\theta^{(0)}\right), \tag{12}$$

where $\tilde{B}_\theta^{(0)} = \tilde{E}_r^{(0)}/c$ is the paraxial and slowly varying envelope of the azimuthal magnetic flux. As we see, it cannot be reduced to a simple expression, as in the case for monochromatic transverse-electromagnetic (TEM) waves [for example, see Eq. 7.11 of Ref. 6].

D. Convergence of the Series

The reader familiar with the type of problem we dealt with in Subsections 2.A–2.C may have recognized a generalization of the previous work of Porras.[8] However, it is known that such series expansions are converging for $1/(\omega_0 T) < 1$ and $1/(k_0 z_R) = 2/(k_0 w_0)^2 < 1$, where T is the pulse duration, $z_R = k_0 w_0^2/2$ is the Rayleigh distance, and w_0 is the beam-spot size at the waist (see also Refs. 8–10 and 12). Moreover, Porras has shown that for a pulse with a single-cycle duration ($T = 2\pi/\omega_0$), temporal series truncated to the second order reproduces accurately the exact field obtained by numerical simulations.[8] We then assume that the spatial series truncated to second order, i.e., in terms proportional to $1/(k_0 z_R)^2$, will also reproduce accurately the exact field of beams with $z_R \geqslant 2\pi/k_0$, i.e., for $w_0 \geqslant \lambda_0/(2\sqrt{\pi})$. This assumption is consistent with the results of Lu *et al.*[13]

To close this section, we would like to emphasize the fact that, in the case of pulsed paraxial TM_{01} beams, the mathematical expression for the field components simplifies to

$$\tilde{E}_r = \sum_{n=0}^{\infty}\left(\frac{j}{\omega_0}\right)^n \partial_{t'}^n \partial_{z'}^{n-1}\left(\frac{z'^n}{n!}\partial_{z'}\tilde{E}_r^{(0)}\right), \tag{13a}$$

$$\tilde{E}_z = \sum_{m=0}^{\infty}\sum_{n=0}^{\infty}\left(\frac{j}{\omega_0}\right)^{m+n} \partial_{t'}^{m+n} \partial_{z'}^{n-1}\left(\frac{z'^n}{n!}\partial_{z'}\tilde{E}_z^{(0)}\right), \tag{13b}$$

$$\tilde{B}_\theta = \tilde{E}_r/c, \tag{13c}$$

where $\tilde{E}_r^{(0)}$ and $\tilde{E}_z^{(0)}$ are the fields of order 0, solutions of the paraxial wave equation, and the paraxial divergence equation (see also Refs. 4 and 8). For continuous nonparaxial beams, the field components are given by

$$\tilde{E}_r = \sum_{n=0}^{\infty}\left(\frac{-j}{2k_0}\right)^n \partial_{z'}^{2n-1}\left(\frac{z'^n}{n!}\partial_{z'}\tilde{E}_r^{(0)}\right), \tag{14a}$$

$$\tilde{E}_z = \sum_{m=0}^{\infty}\sum_{n=0}^{\infty}\left(\frac{-j}{k_0}\right)^{m+n} 2^{-n}\partial_{z'}^{2n-1+m}\left(\frac{z'^n}{n!}\partial_{z'}\tilde{E}_z^{(0)}\right), \tag{14b}$$

$$\tilde{B}_\theta = c^{-1}\sum_{p=0}^{\infty}\sum_{n=0}^{\infty}\left(\frac{-j}{k_0}\right)^{p+n} 2^{-n}\partial_{z'}^{2n-1+p}\left(\frac{z'^n}{n!}\partial_{z'}\tilde{E}_r^{(0)}\right). \tag{14c}$$

3. TIGHT FOCUSING OF AN ULTRAFAST TM_{01} BEAM

A TM_{01} beam can be generated interferometrically by two cross-polarized TEM_{10} and TEM_{01} Gauss–Hermite modes of identical waists.[2,14,15] This particular type of beam thus belongs to the wide family of the Gauss–Hermite beam modes that constitutes, with the Gauss–Laguerre and Gauss–Ince[16–18] beam modes, the mathematical basis for the decomposition of paraxial optical beams.[3,12,19,20] Using the general method presented in Section 2, the validity of these solutions can be extended to ultrafast nonparaxial beams. We here consider the case of an ultrafast TM_{01} beam that is tightly focused by an ideal lens that is corrected for any type of aberration. Special attention is paid to the effects of the spatiotemporal corrections on the longitudinal electric field component.

A. Field Distribution of the Pulsed Tightly Focused TM_{01} Laser Beam

When the transverse dimension at the waist of a TM_{01} beam approaches the central wavelength of the signal, the distribution of the field differs from what is expected from paraxial theory. To proceed with the analysis of this situation, let us consider the focusing of a TM_{01} beam, as shown schematically in Fig. 1. The zeroth-order components of the field before and after the lens are defined as follows:

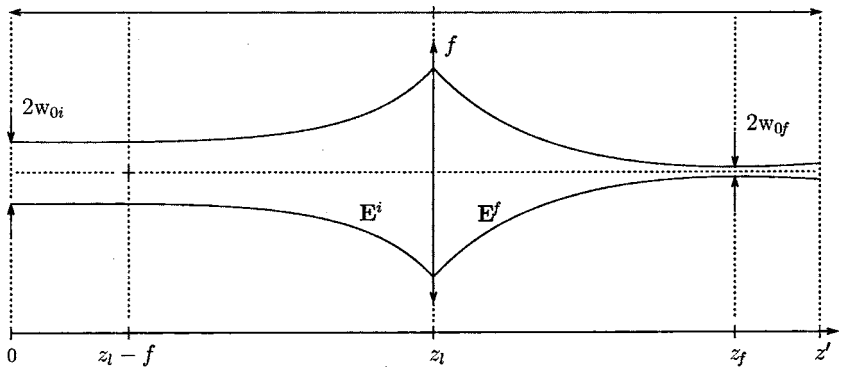

Fig. 1. Schematic representation of the focusing of a pulsed TM_{01} beam. The waist of the entrance beam $\mathbf{E}^i$ is located at $z'=0$, the focusing optics with a given focal length f is placed at $z'=z_l$, and the output beam $\mathbf{E}^f$ has its waist at $z'=z_f$.

$$\tilde{E}_r^{i(0)} = E_{0i}\exp(1/2)\left(\frac{jz_{Ri}}{\tilde{q}_i}\right)^2\frac{\sqrt{2}r}{w_{0i}}\exp\left(-j\frac{k_0r^2}{2\tilde{q}_i}\right)g_i(t'), \tag{15a}$$

$$\tilde{E}_z^{i(0)} = -2jE_{0i}\exp(1/2)\left(\frac{jz_{Ri}}{\tilde{q}_i}\right)^2\frac{\sqrt{2}}{k_0w_{0i}}\left(1-j\frac{k_0r^2}{2\tilde{q}_i}\right)\times\exp\left(-j\frac{k_0r^2}{2\tilde{q}_i}\right)g_i(t'), \tag{15b}$$

$$\tilde{B}_\theta^{i(0)} = \tilde{E}_r^{i(0)}/c, \tag{15c}$$

$$\tilde{E}_r^{f(0)} = E_{0f}\exp(1/2)\left(\frac{jz_{Rf}}{\tilde{q}_f}\right)^2\frac{\sqrt{2}r}{w_{0f}}\exp\left(-j\frac{k_0r^2}{2\tilde{q}_f}\right)g_f(t'), \tag{15d}$$

$$\tilde{E}_z^{f(0)} = -2jE_{0f}\exp(1/2)\left(\frac{jz_{Rf}}{\tilde{q}_f}\right)^2\frac{\sqrt{2}}{k_0w_{0f}}\left(1-j\frac{k_0r^2}{2\tilde{q}_f}\right)\times\exp\left(-j\frac{k_0r^2}{2\tilde{q}_f}\right)g_f(t'), \tag{15e}$$

$$\tilde{B}_\theta^{f(0)} = \tilde{E}_r^{f(0)}/c, \tag{15f}$$

where E_{0i} and E_{0f} are the amplitudes of the transverse field, $\tilde{q}_i=z'+jz_{Ri}$ and $\tilde{q}_f=\Delta z'+jz_{Rf}$ are the complex parameters of the Gaussian beam with $\Delta z'=z'-z_f$ being the distance relative to the waist of the output beam located at $z'=z_f$, $z_{Ri}=k_0w_{0i}^2/2$ and $z_{Rf}=k_0w_{0f}^2/2$ are the Rayleigh distances, $2w_{0i}$ and $2w_{0f}$ are the beam-spot diameters at the entrance waist ($z'=0$) and the output waist ($z'=z_f$), $g_i(t')=\exp(-t'^2/T_i^2)$ and $g_f(t')=\exp(-t'^2/T_f^2)$ are Gaussian pulse envelopes, and T_i and T_f are the pulse durations. The superscripts i (initial) and f (final) refer to the entrance and output fields, respectively.

To guarantee continuity, the beam intensity distributions must match at $z'=z_l$. As a mathematical condition, we impose that the two beams should be of equal size at $z'=z_l$, i.e., $w_i(z_l)=w_f(z_l)$. Thus,

$$w_{0i}\left[1+\left(\frac{z_l}{z_{Ri}}\right)^2\right]^{1/2} = w_{0f}\left[1+\left(\frac{z_l-z_f}{z_{Rf}}\right)^2\right]^{1/2}. \tag{16}$$

If the lens is in the far field of the entrance beam, i.e., $z_l \gg z_{Ri}$, it can be assumed that the incoming wavefront is flat and that the waist of the output beam is in the focal plane of the lens, at $z_f=z_l+f$. Then, if the focal length f is chosen so that the output beam is focused in the far field ($f \gg z_{Rf}$), the beam-spot radius at the waist and the Rayleigh distance of the output beam are given by the following expressions:

$$w_{0f} \simeq w_{0i}(f/z_l), \tag{17a}$$

$$z_{Rf} \simeq z_{Ri}(f/z_l)^2. \tag{17b}$$

It is known that, for beam waists larger than many wavelengths and pulse durations longer than many optical cycles, the field of the pulsed TM_{01} beam is well represented by its zeroth-order components[3,20] given in Eqs. (15a)–(15f). In the case of an ultrafast tightly focused beam, spatiotemporal corrections must be considered, according to the formalism we developed in Section 2. However, we emphasize the fact that for pulse durations longer than two optical cycles, i.e., for $T_f \geqslant 4\pi/\omega_0$ (this corresponds to a pulse duration longer than 5 fs for $\lambda_0=0.8\ \mu$m), the field is described with a fairly good accuracy by the first-order expressions, where the series of corrections is truncated to terms proportional to $(\omega_0^{-1})\partial_{t'}$.[8,13,21] Similarly, in the nonparaxial regime the first spatial correction—proportional to $(k_0^{-1})\partial_{z'}$—will be reasonably smaller than unity for $z_{Rf} \geqslant 4\pi/k_0$, i.e., for $w_{0f} \geqslant (\pi/2)^{-1/2}\lambda_0$ (corresponding to $w_{0f} \simeq 0.64\ \mu$m for $\lambda_0=0.8\ \mu$m). Using the zeroth-order fields defined in Eqs. (15a)–(15f), we calculated the first-order paraxial (before the lens) and nonparaxial (after the lens) envelopes of the ultrafast TM_{01} beam, which are

$$\tilde{E}_r^i \simeq \tilde{E}_r^{i(0)} + j\omega_0^{-1}z'\partial_{t'}\partial_{z'}\tilde{E}_r^{i(0)}, \tag{18a}$$

$$\simeq \tilde{E}_r^{i(0)}\left[1+\frac{2jz't'}{\omega_0T_i^2}\left(\frac{2}{\tilde{q}_i}-\frac{jk_0r^2}{2\tilde{q}_i^2}\right)\right], \tag{18b}$$

$$\tilde{E}_z^i \simeq \tilde{E}_z^{i(0)} + j\omega_0^{-1}\partial_{t'}\tilde{E}_z^{i(0)} + j\omega_0^{-1}z'\partial_{t'}\partial_{z'}\tilde{E}_z^{i(0)}, \tag{18c}$$

$$\simeq \tilde{E}_z^{i(0)}\left[1-\frac{2jt'}{\omega_0 T_i^2}+\frac{2jz't'}{\omega_0 T_i^2}\left(1-\frac{jk_0r^2}{2\tilde{q}_i}\right)^{-1}\times\left(\frac{2}{\tilde{q}_i}-\frac{2jk_0r^2}{\tilde{q}_i^2}-\frac{k_0^2r^4}{4\tilde{q}_i^3}\right)\right], \tag{18d}$$

$$\tilde{B}_\theta^i \simeq \tilde{E}_r^i/c, \tag{18e}$$

$$\simeq \tilde{B}_\theta^{i(0)}\left[1+\frac{2jz't'}{\omega_0 T_i^2}\left(\frac{2}{\tilde{q}_i}-\frac{jk_0r^2}{2\tilde{q}_i^2}\right)\right], \tag{18f}$$

$$\tilde{E}_r^f \simeq \tilde{E}_r^{f(0)}+j\omega_0^{-1}\Delta z'\partial_{t'}\partial_{z'}\tilde{E}_r^{f(0)} - j(2k_0)^{-1}(\partial_{z'}\tilde{E}_r^{f(0)}+\Delta z'\partial_{z'}^2\tilde{E}_r^{f(0)}), \tag{18g}$$

$$\simeq \tilde{E}_r^{f(0)}\left[1+\left(\frac{j}{2k_0}+\frac{2j\Delta z't'}{\omega_0 T_f^2}\right)\left(\frac{2}{\tilde{q}_f}-\frac{jk_0r^2}{2\tilde{q}_f^2}\right)-\frac{j\Delta z'}{2k_0}\left(\frac{6}{\tilde{q}_f^2}-\frac{3jk_0r^2}{\tilde{q}_f^3}-\frac{k_0^2r^4}{4\tilde{q}_f^4}\right)\right], \tag{18h}$$

$$\tilde{E}_z^f \simeq \tilde{E}_z^{f(0)}+j\omega_0^{-1}\partial_{t'}\tilde{E}_z^{f(0)}-jk_0^{-1}\partial_{z'}\tilde{E}_z^{f(0)}+j\omega_0^{-1}\Delta z'\partial_{t'}\partial_{z'}\tilde{E}_z^{f(0)} - j(2k_0)^{-1}(\partial_{z'}\tilde{E}_z^{f(0)}+\Delta z'\partial_{z'}^2\tilde{E}_z^{f(0)}), \tag{18i}$$

$$\simeq \tilde{E}_z^{f(0)}\left[1-\frac{2jt'}{\omega_0 T_f^2}+\left(1-\frac{jk_0r^2}{2\tilde{q}_f}\right)^{-1}\left(\frac{3j}{2k_0}+\frac{2j\Delta z't'}{\omega_0 T_f^2}\right)\times\left(\frac{2}{\tilde{q}_f}-\frac{2jk_0r^2}{\tilde{q}_f^2}-\frac{k_0^2r^4}{4\tilde{q}_f^3}\right)-\frac{j\Delta z'}{2k_0}\left(1-\frac{jk_0r^2}{2\tilde{q}_f}\right)^{-1}\times\left(\frac{6}{\tilde{q}_f^2}-\frac{9jk_0r^2}{\tilde{q}_f^3}-\frac{9k_0^2r^4}{4\tilde{q}_f^4}+\frac{jk_0^3r^6}{8\tilde{q}_f^5}\right)\right], \tag{18j}$$

$$\tilde{B}_\theta^f \simeq \tilde{B}_\theta^{f(0)}-jk_0^{-1}\partial_{z'}\tilde{B}_\theta^{f(0)}+j\omega_0^{-1}\Delta z'\partial_{t'}\partial_{z'}\tilde{B}_\theta^{f(0)} - j(2k_0)^{-1}(\partial_{z'}\tilde{B}_\theta^{f(0)}+\Delta z'\partial_{z'}^2\tilde{B}_\theta^{f(0)}), \tag{18k}$$

$$\simeq \tilde{B}_\theta^{f(0)}\left[1+\left(\frac{3j}{2k_0}+\frac{2j\Delta z't'}{\omega_0 T_f^2}\right)\left(\frac{2}{\tilde{q}_f}-\frac{jk_0r^2}{2\tilde{q}_f^2}\right)-\frac{j\Delta z'}{2k_0}\left(\frac{6}{\tilde{q}_f^2}-\frac{3jk_0r^2}{\tilde{q}_f^3}-\frac{k_0^2r^4}{4\tilde{q}_f^4}\right)\right]. \tag{18l}$$

In Fig. 2, the first-order components given in Eqs. (18a)–(18l) are compared with the zeroth-order components for $t'=0$ and various positions along the propagation axis. It is thus observed that for $w_{0f}\geqslant 3\lambda_0$ the spatial corrections are negligible, as shown in Fig. 2(b). On the other hand, when the beam radius at the waist w_{0f} is of the order of the central wavelength λ_0, the first-order corrections produce a substantial increase of the longitudinal field in the vicinity of the focus. This result can be interpreted in terms of plane waves coming from the outer part of the beam, neglected in the paraxial approximation, as seen in Fig. 2(a). When these contributions reach the focus, where they cross the z' axis, the longitudinal projections of their respective electric field vectors interfere constructively at $r=0$, thus locally increasing the strength of the longitudinal field. As we will immediately see, when the beam-spot diameter at the waist is comparable to the wavelength, the spatial corrections involve important modifications of beam structure, mostly in the focal region.[22]

According to the work of Porras,[8] and by the analogy between the spatial and temporal series of Eq. (9), spatial corrections up to the second order must be introduced to deal with the propagation of a TM_{01} beam whose Rayleigh distance is on the scale of a wavelength. At the waist ($z'=z_f$), for continuous signals or when the temporal envelope has a duration of several optical cycles, the second-order components of the nonparaxial output field are given by the following equations:

$$\tilde{E}_r^f(z'=z_f) \simeq [\tilde{E}_r^{f(0)}]_{z'=z_f}\left[1+(k_0w_{0f})^{-2}\left(2-\frac{r^2}{w_{0f}^2}\right)+(k_0w_{0f})^{-4}\left(18-\frac{32r^2}{w_{0f}^2}+\frac{3r^4}{w_{0f}^4}\right)\right], \tag{19a}$$

$$\tilde{E}_z^f(z'=z_f) \simeq [\tilde{E}_z^{f(0)}]_{z'=z_f}\left[1+6(k_0w_{0f})^{-2}\left(1-\frac{r^2}{w_{0f}^2}\right)+\frac{33}{2}(k_0w_{0f})^{-4}\left(1-\frac{r^2}{w_{0f}^2}\right)^{-1}\left(1-\frac{12r^2}{w_{0f}^2}+\frac{6r^4}{w_{0f}^4}-\frac{2r^6}{3w_{0f}^6}\right)\right], \tag{19b}$$

$$\tilde{B}_\theta^f(z'=z_f) \simeq c^{-1}[\tilde{E}_r^{f(0)}]_{z'=z_f}\left[1+3(k_0w_{0f})^{-2}\left(2-\frac{r^2}{w_{0f}^2}\right)+\frac{11}{3}(k_0w_{0f})^{-4}\left(18-\frac{32r^2}{w_{0f}^2}+\frac{3r^4}{w_{0f}^4}\right)\right], \tag{19c}$$

where

$$[\tilde{E}_r^{f(0)}]_{z'=z_f}=\frac{E_{0f}\exp(1/2)\sqrt{2}}{w_{0f}}r\exp\left(-\frac{r^2}{w_{0f}^2}\right)g_f(t'), \tag{20a}$$

$$[\tilde{E}_z^{f(0)}]_{z'=z_f}=-2j\frac{E_{0f}\exp(1/2)\sqrt{2}}{k_0w_{0f}}\left(1-\frac{r^2}{w_{0f}^2}\right)\times\exp\left(-\frac{r^2}{w_{0f}^2}\right)g_f(t'). \tag{20b}$$

From these expressions, we define u_i and u_f, the mean energy density of the entrance and output beams, as follows (see Section 6.9 of Ref. 6):

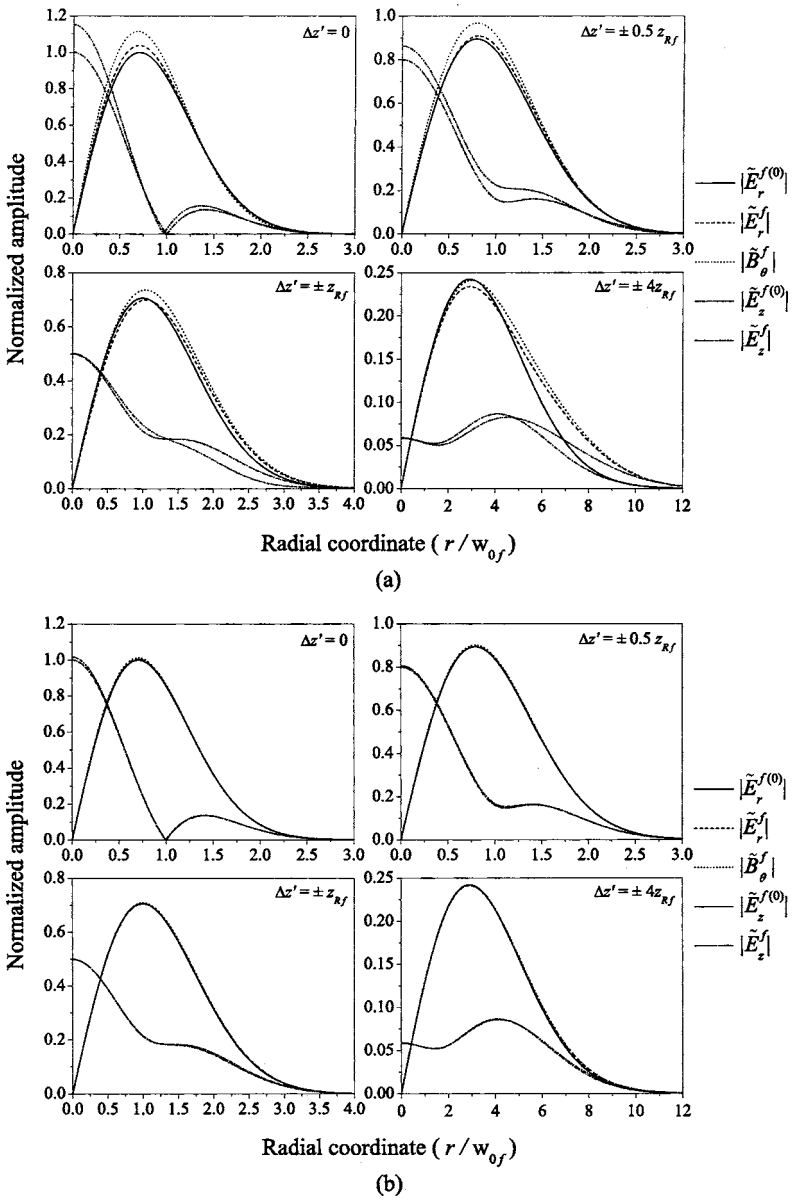

Fig. 2. Radial distribution of the zeroth-order (superscript 0) and first-order envelopes of the field components of a TM_{01} beam at different positions along the z' axis for $t'=0$, as defined in Eqs. (15) and (18). (a) $w_{0f}=\lambda_0$ and (b) $w_{0f}=3\lambda_0$. Fields are not to scale; they have been normalized so that the maximum value of their respective zeroth-order expression is equal to 1 at the waist ($\Delta z'=0$). It should be noticed that at $t'=0$, the first-order expressions for the field components do not depend upon T_f.

$$u_i \simeq \frac{\epsilon_0}{4}(|\tilde{E}_r^i|^2 + c^2|\tilde{B}_\theta^i|^2) = \frac{\epsilon_0}{2}|\tilde{E}_r^{i(0)}|^2, \tag{21a}$$

$$u_f = \frac{\epsilon_0}{4}(|\tilde{E}_r^f|^2 + |\tilde{E}_z^f|^2 + c^2|\tilde{B}_\theta^f|^2). \tag{21b}$$

After the integration of these densities, the energy of the pulse is obtained before and after the lens, i.e.,

$$W_i = \frac{E_{0i}^2}{2\eta_0}\left(\frac{\pi}{2}\right)^{3/2} w_{0i}^2 T_i \exp(1), \tag{22a}$$

$$W_f = \frac{E_{0f}^2}{2\eta_0}\left(\frac{\pi}{2}\right)^{3/2} w_{0f}^2 T_f \exp(1)\left[1 + 6(k_0 w_{0f})^{-2} - \frac{149}{6}(k_0 w_{0f})^{-4} + 30(k_0 w_{0f})^{-6} + \frac{13\,289}{6}(k_0 w_{0f})^{-8} + 11\,979(k_0 w_{0f})^{-10}\right], \tag{22b}$$

with η_0 being the intrinsic impedance of free space. If the losses due to the lens are negligible, the conservation of energy implies $W_i = W_f$. Thus, E_{0f} is isolated to give

$$E_{0f} = E_{0i}\left(\frac{w_{0i}}{w_{0f}}\right)\left(\frac{T_i}{T_f}\right)^{1/2}\left[1 + 6(k_0 w_{0f})^{-2} - \frac{149}{6}(k_0 w_{0f})^{-4} + 30(k_0 w_{0f})^{-6} + \frac{13\,289}{6}(k_0 w_{0f})^{-8} + 11\,979(k_0 w_{0f})^{-10}\right]^{-1/2}, \quad (23)$$

which guarantees the conservation of energy for the second-order fields given in relations (19).

The contribution of each component to the total power of the beam is given in Fig. 3. It is observed that for a paraxial TM_{01} beam—whose longitudinal field is vanishingly small—the total power is equally distributed between the radial electric field and the azimuthal magnetic field. However, when the spot size approaches the wavelength, a significant fraction of the total power is given to the longitudinal electric field, while the power stored in the transverse-electric and transverse-magnetic components decreases. For $w_{0f} < 0.5\lambda_0$, the power of the longitudinal field becomes more important than that of the transverse field, which explains the presence of a bright spot at the center of the beam (see Fig. 4 of this paper and Figs. 2 and 3 of Ref. 2). Hence it clearly stands out that there is an exchange of energy between the transverse fields and the longitudinal field (the origin of this phenomenon is predominantly geometric, however).

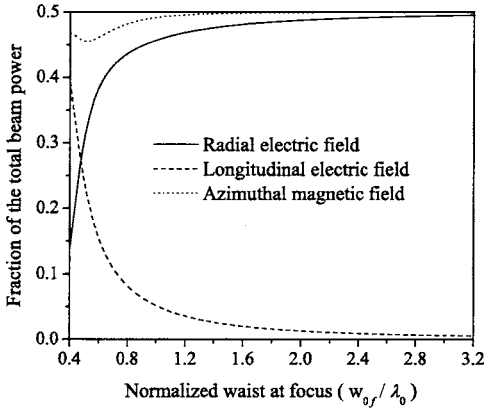

Fig. 3. Fraction of the total beam power stored in the components of a continuous TM_{01} beam at the waist ($z' = z_f$).

In their experiment, Dorn *et al.*[2] measured the electric energy density of strongly focused TM_{01} beams, which is

$$u_{ef} = \frac{\epsilon_0}{4}|\tilde{\mathbf{E}}^f|^2 = \frac{\epsilon_0}{4}(|\tilde{E}_r^f|^2 + |\tilde{E}_z^f|^2). \quad (24)$$

As they stated, this is the part of the field that couples to standard detectors and photosensitive materials. Consequently, the measured intensity of the output field is defined as follows:

$$I_f = cu_{ef}, \quad (25a)$$

$$= \frac{|\tilde{E}_r^f|^2 + |\tilde{E}_z^f|^2}{4\eta_0}. \quad (25b)$$

The measured beam power would thus be the surface integral of the intensity in the plane perpendicular to the average Poynting vector. However, from the fields given in Eqs. (15), (18), and (19)—i.e., from the zeroth-, first-, and second-order fields—the zeroth-, first-, and second-order intensities are defined, respectively. These are compared in Fig. 4. It is thus observed that when w_{0f} is large with regard to the wavelength, i.e., when $w_{0f} \gg \lambda_0$, the beam profile is the usual doughnut-like shape predicted by paraxial theory.[3] On the other hand, when w_{0f} approaches and becomes smaller than the wavelength, the growing presence of the longitudinal field changes the beam profile that evolves from the doughnut shape to a flattop beam and, finally, to a beam with a sharp peak at the cen-

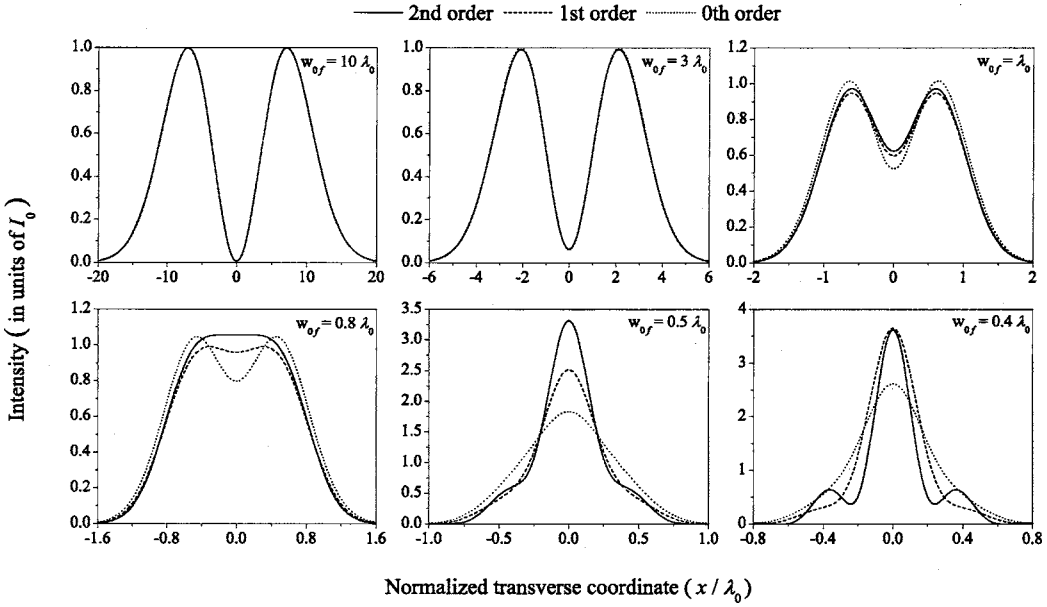

Fig. 4. Zeroth-, first-, and second-order intensities of a continuous TM_{01} beam at $z' = z_f$ for various beam-spot sizes (given in each graph). The intensity of each curve is normalized so that the total power is conserved and is given in units of $I_0 = E_{0i}^2(\pi/2)^{3/2}\exp(1)/2\eta_0$.

ter. It is here observed that the zeroth-order intensity gives an accurate evaluation of the field for $w_{0f} \geqslant 3\lambda_0$. This is consistent with what has been shown in Fig. 2. Furthermore, for $w_{0f}=0.8\lambda_0$ the first-order intensity perfectly overlaps the second-order curve, but not at the center of the beam. For $w_{0f}=0.5\lambda_0$, calculations clearly predict a narrow peak at the center of the beam, as reported by Dorn *et al.*[2] It is observed that the paraxial approximation tends to underestimate its strength. The predicted spot size ($0.11\lambda_0^2$) inferred from the second-order intensity profile is lower than the value ($0.16\lambda_0^2$) reported by Dorn *et al.*; this could be due to the fact that we have used an ideal beam profile (TM_{01}) while, in a real experiment, unfiltered higher-order TM modes are present and their contribution broadens the beam spot size. For $w_{0f}=0.4\lambda_0$ it is observed that the transfer of power to the longitudinal electric component is saturated and that extra energy is stored in off-axis oscillations (see also Ref. 22).

In light of what we have seen in this subsection, there is no doubt that the paraxial approximation is not appropriate to deal with TM_{01} beams with large divergence angles. However, corrections of the first and second orders have been extensively calculated here. Consequently, it is observed that when a TM_{01} beam is tightly focused, an important fraction of the total power is transferred to the longitudinal electric field without affecting the characteristic azimuthal symmetry of the beam. We recall that this particular behavior is consistent with the experimental results obtained by Dorn *et al.*[2] We will now study this axial longitudinal electric field in detail for a pulse with an ultrashort duration.

B. Axial Longitudinal Electric Field of the Few-Cycle Tightly Focused TM_{01} Beam

The longitudinal electric field of the TM_{01} beam reaches its maximum amplitude at the center of the beam, where that of the other components is null (see Fig. 2). This particular feature is quite interesting for the acceleration of charged particles in free space.[4] However, using Eqs. (10) and (15e), the second-order longitudinal electric field of a few-cycle TM_{01} beam at $r=0$ is defined as follows:

$$\begin{aligned}\tilde{\mathbb{E}}_z^f = \tilde{\mathbb{E}}_z^{f(0)}\Bigg[& 1 - \frac{2jt'}{\omega_0 T_f^2}\left(1 - \frac{2\Delta z'}{\tilde{q}_f}\right) + \frac{3j}{k_0\tilde{q}_f}\left(1 - \frac{\Delta z'}{\tilde{q}_f}\right) \\ & - \frac{2}{\omega_0^2 T_f^2}\left(1 - \frac{2t'^2}{T_f^2}\right)\left(\frac{4\Delta z'}{\tilde{q}_f} - \frac{3\Delta z'^2}{\tilde{q}_f^2}\right) \\ & + \frac{2t'}{k_0\omega_0 T_f^2\tilde{q}_f}\left(5 - \frac{12\Delta z'}{\tilde{q}_f} + \frac{12\Delta z'^2}{\tilde{q}_f^2}\right) \\ & - \frac{3}{2k_0^2\tilde{q}_f^2}\left(7 - \frac{20\Delta z'}{\tilde{q}_f} + \frac{10\Delta z'^2}{\tilde{q}_f^2}\right)\Bigg],\end{aligned} \tag{26}$$

where the axial zeroth-order field is given by

$$\tilde{\mathbb{E}}_z^{f(0)} = -2jE_{0f}\exp(1/2)\frac{\sqrt{2}}{k_0 w_{0f}}\left(\frac{jz_{Rf}}{\tilde{q}_f}\right)^2 \exp(-t'^2/T_f^2), \tag{27}$$

and the physical axial field is as follows:

$$\mathbb{E}_z^f = \mathrm{Re}[\tilde{\mathbb{E}}_z^f \exp(j\omega_0 t')]. \tag{28}$$

This suggests that the complex amplitude $\tilde{\mathbb{E}}_z^f$ can be written as

$$\tilde{\mathbb{E}}_z^f = \tilde{\mathbb{E}}_z^{f(0)}\tilde{\Omega} \tag{29a}$$

$$= |\tilde{\mathbb{E}}_z^{f(0)}||\tilde{\Omega}|\exp(2j\Phi_G + j\Phi_C - j\pi/2), \tag{29b}$$

where

$$|\tilde{\mathbb{E}}_z^{f(0)}| = 2E_{0f}\exp(1/2)\frac{\sqrt{2}}{k_0 w_{0f}}\left(\frac{w_{0f}}{w_f(z')}\right)^2 \exp(-t'^2/T_f^2), \tag{30a}$$

$$\Phi_G = \tan^{-1}(\Delta z'/z_{Rf}), \tag{30b}$$

with $w_f(z')=w_{0f}(1+\Delta z'^2/z_{Rf}^2)^{1/2}$. The complex function $\tilde{\Omega} = |\tilde{\Omega}|\exp(j\Phi_C)$ refers to the terms in the square brackets of Eq. (26). After manipulations, it is shown that

$$\begin{aligned}\mathrm{Re}[\tilde{\Omega}] = 1 & + \frac{4t'Z'}{\omega_0 T_f^2(1+Z'^2)} + \frac{3(1-Z'^2)}{k_0 z_{Rf}(1+Z'^2)^2} \\ & - \frac{2}{(\omega_0 T_f)^2}\left(1 - \frac{2t'^2}{T_f^2}\right)\frac{(7Z'^2+Z'^4)}{(1+Z'^2)^2} \\ & + \frac{2t'}{k_0 z_{Rf}\omega_0 T_f^2}\frac{Z'(17-26Z'^2+5Z'^4)}{(1+Z'^2)^3} \\ & + \frac{3}{2(k_0 z_{Rf})^2}\frac{(7-63Z'^2+13Z'^4+3Z'^6)}{(1+Z'^2)^4},\end{aligned} \tag{31a}$$

$$\begin{aligned}\mathrm{Im}[\tilde{\Omega}] = & -\frac{2t'}{\omega_0 T_f^2}\left(\frac{1-Z'^2}{1+Z'^2}\right) + \frac{6Z'}{k_0 z_{Rf}(1+Z'^2)^2} \\ & + \frac{2}{(\omega_0 T_f)^2}\left(1 - \frac{2t'^2}{T_f^2}\right)\frac{(4Z'-2Z'^3)}{(1+Z'^2)^2} \\ & - \frac{2t'}{k_0 z_{Rf}\omega_0 T_f^2}\frac{(5+26Z'^2+17Z'^4)}{(1+Z'^2)^3} \\ & + \frac{3}{(k_0 z_{Rf})^2}\frac{Z'(17-26Z'^2+3Z'^4)}{(1+Z'^2)^4},\end{aligned} \tag{31b}$$

where $Z'=\Delta z'/z_{Rf}$. It is then trivial to obtain the physical field of Eq. (28) in terms of its amplitude and phase.

In a previous publication, we described in detail the longitudinal field of an ultrafast paraxial TM_{01} beam.[4] Similar results—here including the corrections to the paraxial approximation—are shown in Figs. 5 and 6. Again, it is seen that due to the finite duration of the signal, the pulse envelope is faster (negative time delay) before the waist but slowed down (positive time delay) after this position. This effect is negligible for a pulsed beam whose length is of several optical cycles [see Fig. 5(a)] but is more pronounced for single-cycle durations [see Fig. 5(b)]. In addition to this observation are the shift of the carrier frequency and the faster divergence of the trans-

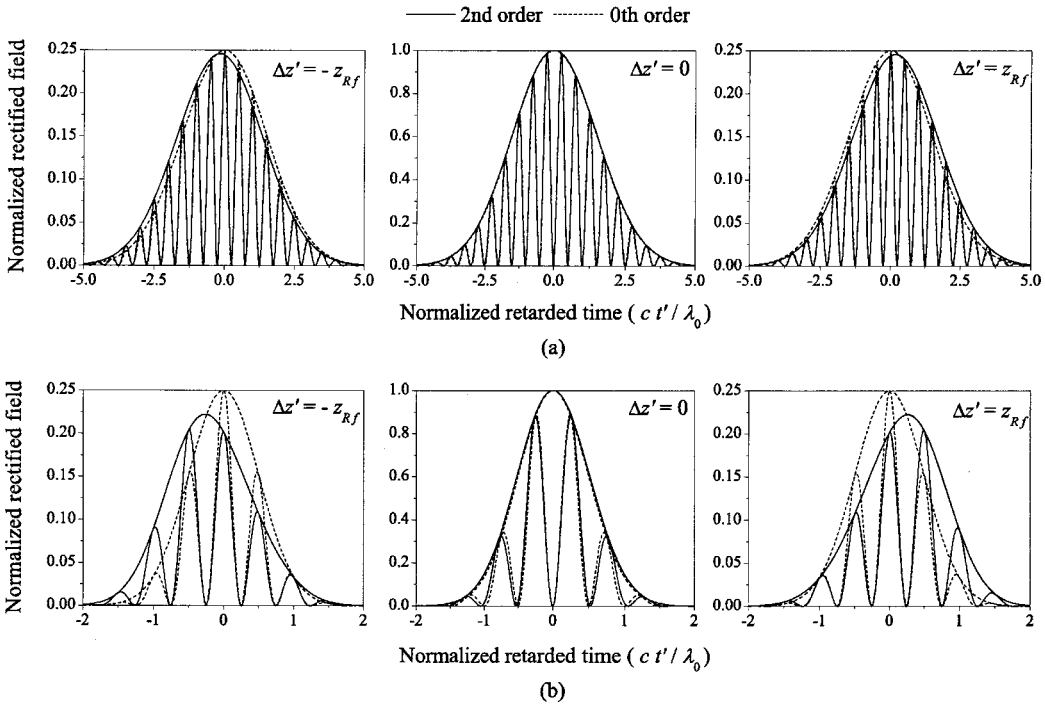

Fig. 5. Temporal distribution of the longitudinal electric field of ultrafast paraxial TM_{01} beams ($w_{0f}=10\lambda_0$) for various positions along the z' axis (at the beam center $r=0$). (a) $T_f=6\pi/\omega_0$ and (b) $T_f=2\pi/\omega_0$. The rectified fields have been normalized so that their envelope is equal to 1 at the center of the pulse ($t'=0$) and at the waist ($\Delta z'=0$). The complex envelope of the second-order field is given in Eq. (26).

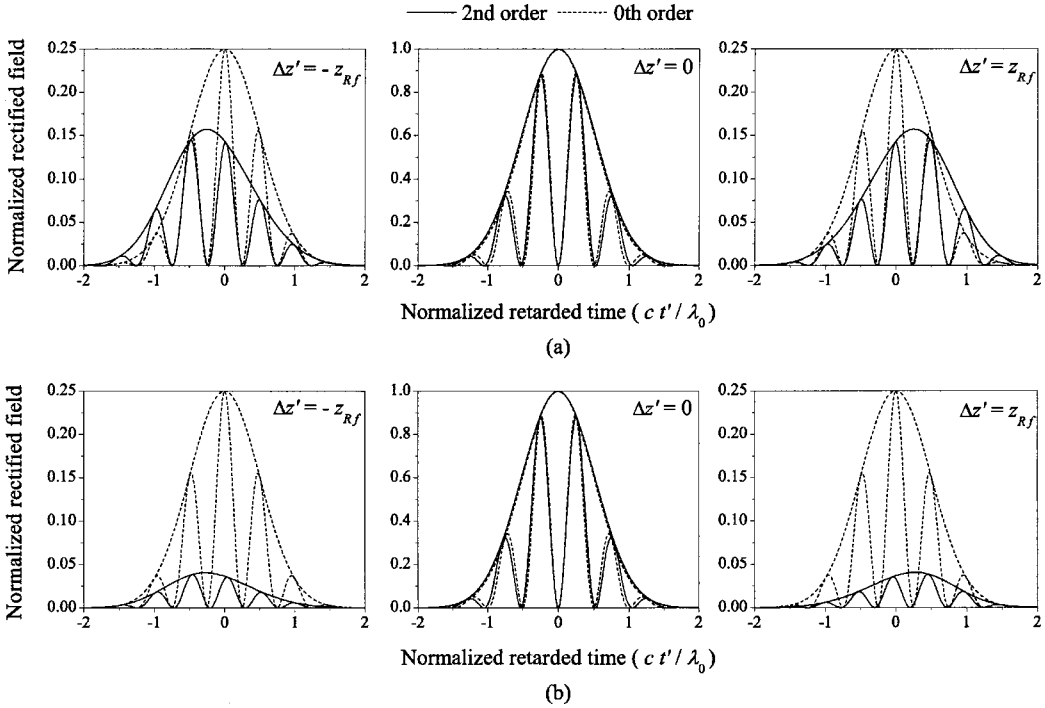

Fig. 6. Temporal distribution of the longitudinal electric field of ultrafast ($T_f=2\pi/\omega_0$) tightly focused TM_{01} beams for various positions along the z' axis (at the beam center $r=0$). (a) $w_{0f}=\lambda_0$ and (b) $w_{0f}=0.5\lambda_0$. See also the caption of Fig. 5.

verse profile away from the waist; both effects are more pronounced for small beam spot sizes, as seen in Fig. 6.

Recalling Eqs. (28) and (29), the total phase of the field is

$$\Phi(Z',t') = \omega_0 t' + 2\Phi_G(Z') + \Phi_C(Z',t') - \pi/2. \quad (32)$$

For a given position along the z' axis, the phase correction Φ_C gives the shift of the carrier frequency inside the

pulse. For example, at the waist (at $Z'=0$), the phase is

$$\Phi(0,t') = \omega_0 t' + \Phi_C(0,t') - \pi/2, \tag{33}$$

which can alternatively be written as

$$\Phi(0,t') = \omega_0' t' - \pi/2, \tag{34}$$

where $\omega_0' = \omega_0 + t'^{-1}\Phi_C(0,t')$. Then, from Eqs. (31) it is shown that the frequency shift at the waist is given by

$$\left(\frac{\omega_0' - \omega_0}{\omega_0}\right)_{Z'=0} = -\frac{1}{\omega_0 t'} \tan^{-1}\left(\frac{2Kt'}{\omega_0 T_f^2}\right), \tag{35}$$

where $K=(1+5/k_0 z_{Rf})/(1+3/k_0 z_{Rf}+21/2k_0^2 z_{Rf}^2)$, or (for small t'):

$$\left(\frac{\omega_0' - \omega_0}{\omega_0}\right)_{Z'=0} \simeq -\frac{2K}{(\omega_0 T_f)^2}\left[1 - \frac{1}{3}\left(\frac{2Kt'}{\omega_0 T_f^2}\right)^2\right]. \tag{36}$$

It is thus observed that, at the waist, the carrier frequency is redshifted. This phenomenon is represented in Fig. 7(a). However, the axial frequency shift of an ultrafast pulsed TM_{01} beam changes with the position along the propagation axis, as reported before.[4] As a result, the carrier wave is redshifted between the beam waist and the Rayleigh distance and blueshifted beyond this position. It is further observed that at $Z'=\pm\infty$ the frequency shift is

$$\left(\frac{\omega_0' - \omega_0}{\omega_0}\right)_{Z'=\pm\infty} = \frac{1}{\omega_0 t'} \tan^{-1}\left(\frac{2t'/\omega_0 T_f^2}{1 - 2/(\omega_0 T_f)^2 + (2t'/\omega_0 T_f^2)^2}\right), \tag{37a}$$

$$\simeq \frac{2/(\omega_0 T_f)^2}{1 - 2/(\omega_0 T_f)^2 + (2t'/\omega_0 T_f^2)^2}, \tag{37b}$$

which represents a distributed blueshift ($\omega_0' > \omega_0$) [see Fig. 7(b)]. It should be noticed that the frequency shift at infinity does not depend upon beam transverse dimensions.

Using the total phase given in Eq. (32), the corrected Gouy phase Φ_{GC} is defined at the center of the pulse ($t'=0$) as follows:

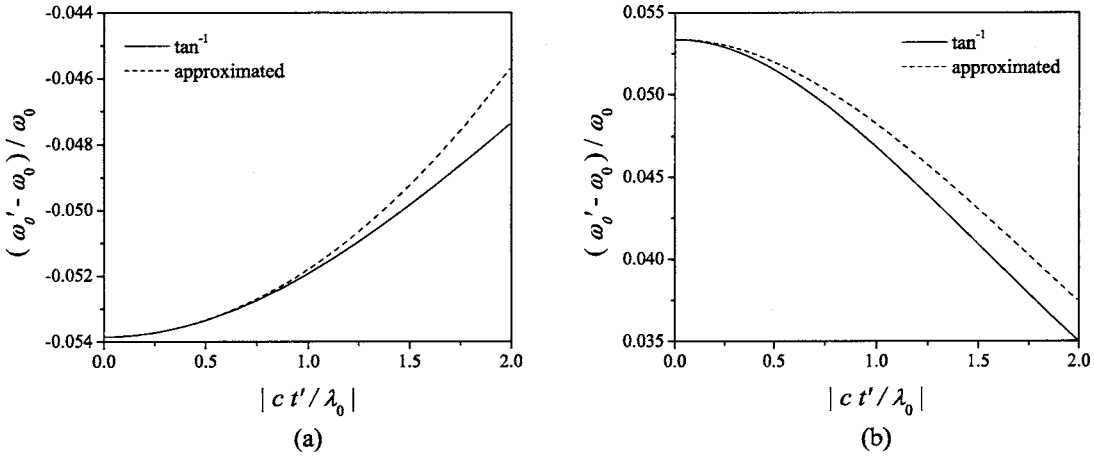

Fig. 7. Axial frequency shift of an ultrafast tightly focused TM_{01} beam ($T_f=2\pi/\omega_0$ and $w_{0f}=\lambda_0$). (a) At the waist ($Z'=0$), the solid curve is Eq. (35) and the dashed curve is relation (36). (b) Far from the waist ($|Z'|\gg 1$), the solid curve is Eq. (37a) and the dashed curve is relation (37b). It should be noticed that in the far field ($|\Delta z'|\gg z_{Rf}$) the frequency shift does not depend upon w_{0f}, the beam-spot size at the waist.

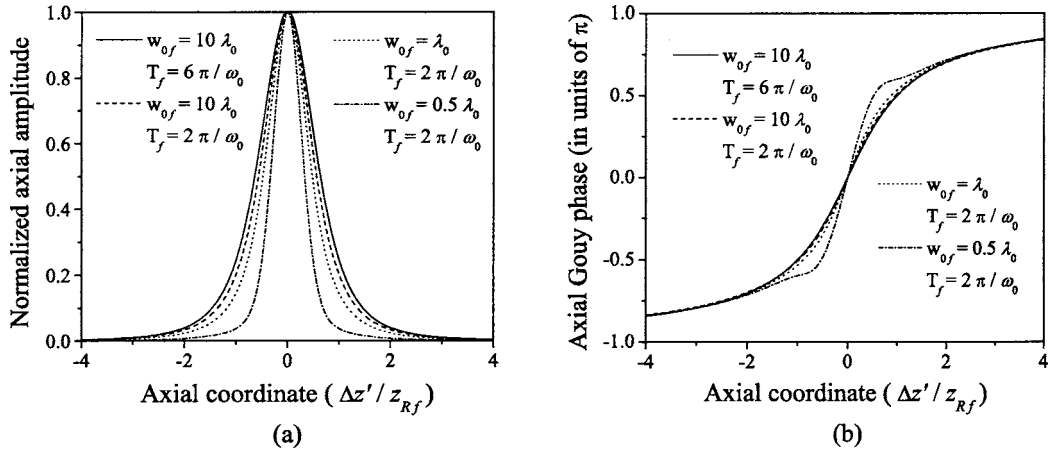

Fig. 8. (a) Normalized amplitude and (b) axial Gouy phase of the longitudinal electric field of an ultrafast tightly focused TM_{01} beam ($t'=0$).

$$\Phi_{GC}(Z') = 2\Phi_G(Z') + \Phi_C(Z',0). \tag{38}$$

It is then straightforward to evaluate the following limits:

$$\Phi_{GC}(Z' = 0) = 0, \tag{39}$$

$$\Phi_{GC}(Z' = \pm\infty) = \pm\pi. \tag{40}$$

It is hence observed that the field experiences an overall phase shift of 2π, twice that of the fundamental Gaussian beam,[23] a result that is independent of the pulse duration and beam-spot size at the waist [see Fig. 8(b)]. On the other hand, one would have noticed, in Fig. 6, the faster decrease of the longitudinal field amplitude away from the waist for small spot sizes. This phenomenon is clearly illustrated in Fig. 8(a), where the amplitude of the longitudinal electric field is given along the z' axis. It is then observed [Fig. 8(b)] that this faster beam divergence is also revealed by a faster variation of the Gouy phase shift near the beam waist, as expected from theory (see Ref. 24). However, we emphasize the fact that this effect is important only for subwavelength spot sizes, i.e., for $w_{0f} < \lambda_0$, and that it takes place within only two Rayleigh distances on each side of the waist [see again Fig. 8(b)].

4. DISCUSSION

In the past, many investigations have been devoted to the study of the paraxial wave equation and its solutions. More specifically, we make reference to the wide family of the Gauss–Hermite, Gauss–Laguerre, and Gauss–Ince beam modes.[3,16,19,20] Using the formalism we have proposed, these solutions—or any solution obtained under the paraxial beam optics theory, just like the TM_{01} beam—can be extended to the case of ultrafast tightly focused pulsed beams.

The method we have presented here is not the unique approach to the problem of tight focusing of ultrafast pulsed beams. Alternatively, a frequency-domain analysis could have been used (see, for example, Refs. 13 and 21; these authors have not considered the case of the TM_{01} beam). An interesting feature of our approach is that it displays directly, in the time domain, the corrections to the four-dimensional structure of the wave packet, as needed to correctly predict ultrafast interactions with matter. Although we think that second-order corrections may be sufficient to deal with most problems, the reader should be aware that in some particular situations, such as in describing the interaction of ultraintense light beams with free charged particles,[25,26] higher-order corrections must be considered. Appropriate series truncation should thus be carefully evaluated regarding the problem at hand.

In this paper, we presented an aberrationless model of the tight focusing of TM_{01} beams. This allowed us to deal with energy conservation and hence to normalize the electromagnetic field of the output beam in terms of the amplitude of the input beam. For several applications this simplified treatment may be unsatisfactory. Effectively, the problem of tight focusing of ultrafast TM_{01} beams is not completely solved unless the aberrations and dispersive properties of the focusing optics are considered. In future works, it might be interesting to characterize nonparaxial transformations of ultrashort paraxial TM_{01} beams by general optical systems in terms of *ABCD* matrices. Nevertheless, we recall that the theoretical results presented in this paper are consistent with the experimental observations reported by Dorn *et al.*[2] and with other theoretical papers dealing with radially polarized beams.[1,15,27] It should be noticed that the temporal effects associated with a tightly focused pulsed TM_{01} beam were not considered in these references. To the best of our knowledge, our paper may be the most detailed description of the propagation of an ultrafast tightly focused TM_{01} beam.

5. CONCLUSION

By means of a purely time-domain method, we solved Maxwell's equations in terms of an infinite series of corrections to a paraxial solution whose temporal envelope varies slowly compared to the carrier oscillations. We have demonstrated the potential of this method by calculating the corrections that apply to an ultrafast tightly focused TM_{01} beam. We observed that the paraxial and the slowly varying envelope approximations underestimate the strength of the longitudinal electric field component in the case of large divergence angles (strong focusing) and ultrashort durations. As a matter of fact, reducing the beam-spot size increases the amplitude of the longitudinal electric field but causes the beam to diverge more rapidly. A consequence of this phenomenon is a faster decrease of the amplitude of the longitudinal field away from the waist. Consequently, the axial Gouy phase shift evolves more rapidly in the vicinity of the focus but keeps its overall variation of 2π from $z=-\infty$ to ∞, as predicted by paraxial theory. We think that these observations would be greatly profitable for two-photon microscopy applications. In fact, two-photon absorption is sensitive to the square of the intensity. According to what we have shown here, a TM_{01} beam with a subwavelength spot size at the waist would illuminate a much smaller sample volume than what was done with a fundamental TEM_{00} Gaussian beam, whose field decreases more slowly away from focus. This would considerably increase the three-dimensional resolution of this type of microscope.

ACKNOWLEDGMENTS

This work has been financially supported by Les Fonds de Recherche sur la Nature et les Technologies (Québec), the Natural Sciences and Engineering Research Council (Canada), and the Canadian Institute for Photonic Innovations.

Corresponding author M. Piché's e-mail address is mpiche@phy.ulaval.ca.

REFERENCES

1. S. Quabis, R. Dorn, M. Eberler, O. Glockl, and G. Leuchs, "Focusing light to a tighter spot," Opt. Commun. **179**, 1–7 (2000).
2. R. Dorn, S. Quabis, and G. Leuchs, "Sharper focus for a radially polarized light beam," Phys. Rev. Lett. **91**, 233901 (2003).
3. A. E. Siegman, *Lasers* (University Science, 1986).

4. C. Varin, M. Piché, and M. A. Porras, "Acceleration of electrons from rest to GeV energies by ultrashort transverse magnetic laser pulses in free space," Phys. Rev. E **71**, 026603 (2005).
5. T. Brabec and F. Krausz, "Intense few-cycle laser fields: frontiers of nonlinear optics," Rev. Mod. Phys. **72**, 545–591 (2000).
6. J. D. Jackson, *Classical Electrodynamics*, 3rd ed. (Wiley, 1999).
7. T. Brabec and F. Krausz, "Nonlinear optical pulse propagation in the single-cycle regime," Phys. Rev. Lett. **78**, 3282–3285 (1997).
8. M. A. Porras, "Pulse correction to monochromatic light-beam propagation," Opt. Lett. **26**, 44–46 (2001).
9. G. P. Agrawal and M. Lax, "Free-space wave propagation beyond the paraxial approximation," Phys. Rev. A **27**, 1693–1695 (1983).
10. M. Lax, W. H. Louisell, and W. B. McKnight, "From Maxwell to paraxial wave optics," Phys. Rev. A **11**, 1365–1370 (1975).
11. E. H. Haselhoff, "Free-electron-laser model without the slowly-varying-envelope approximation," Phys. Rev. E **49**, R47–R50 (1994).
12. L. W. Davis, "Theory of electromagnetic beams," Phys. Rev. A **19**, 1177–1179 (1979).
13. D. Lu, W. Hu, Y. Zheng, and Z. Yang, "Propagation of pulsed beam beyond the paraxial approximation in free space," Opt. Commun. **228**, 217–223 (2003).
14. S. Tidwell, D. H. Ford, and D. Kimura, "Generating radially polarized beams interferometrically," Appl. Opt. **29**, 2234–2239 (1990).
15. K. S. Youngworth and T. G. Brown, "Focusing of high numerical aperture cylindrical-vector beams," Opt. Express **7**, 77–87 (2000).
16. M. A. Bandres and J. C. Gutierrez-Vega, "Ince–Gaussian modes of the paraxial wave equation and stable resonators," J. Opt. Soc. Am. A **21**, 873–880 (2004).
17. M. A. Bandres, "Elegant Ince–Gaussian beams," Opt. Lett. **29**, 1724–1726 (2004).
18. U. T. Schwarz, M. A. Bandres, and J. C. Gutierrez-Vega, "Observation of Ince–Gaussian modes in stable resonators," Opt. Lett. **29**, 1870–1872 (2004).
19. L. W. Davis, "Vector electromagnetic modes of an optical resonator," Phys. Rev. A **30**, 3092–3096 (1984).
20. W. L. Erikson and S. Singh, "Polarization properties of Maxwell-Gaussian laser beams," Phys. Rev. E **49**, 5778–5786 (1994).
21. D. Lu, W. Hu, Z. Yang, and Y. Zheng, "Vectorial nature of nonparaxial ultrashort pulsed beam," J. Opt. A, Pure Appl. Opt. **5**, 263–267 (2003).
22. W. H. Carter, "Anomalies in the field of a gaussian beam near focus," Opt. Commun. **7**, 211–218 (1973).
23. F. Lindner, G. G. Paulus, H. Walther, A. Baltuška, E. Goulielmakis, M. Lezius, and F. Krausz, "Gouy phase shift for few-cycle laser pulses," Phys. Rev. Lett. **92**, 113001 (2004).
24. S. Feng and H. G. Winful, "Physical origin of the Gouy phase shift," Opt. Lett. **26**, 485–487 (2001).
25. H. Hora, M. Hoelss, W. Scheid, J. W. Wang, Y. K. Ho, F. Osman, and R. Castillo, "Principle of high accuracy for the nonlinear theory of the acceleration of electrons in a vacuum by lasers at relativistic intensities," Laser Part. Beams **18**, 135–144 (2000).
26. N. Cao, Y. K. Ho, Q. Kong, P. X. Wang, X. Q. Yuan, Y. Nishida, N. Yugami, and H. Ito, "Accurate description of Gaussian laser beams and electron dynamics," Opt. Commun. **204**, 7–15 (2002).
27. M. O. Scully and M. S. Zubairy, "Simple laser accelerator: optics and particle dynamics," Phys. Rev. A **44**, 2656–2663 (1991).